THE JOURNAL OF BIOLOGICAL CHEMISTRY VOL. 279, NO. 47, ISSUE OF NOVEMBER 19, pp. 48647–48653, 2004

Printed in U.S.A.

Recoverin and Rhodopsin Kinase Activity in Detergent-resistant Membrane Rafts from Rod Outer Segments*

Received for publication, March 5, 2004, and in revised form, August 30, 2004
Published, JBC Papers in Press, September 7, 2004, DOI 10.1074/jbc.M402516200

Ivan I. Senin‡, Doris Höppner-Heitmann§, Olga O. Polkovnikova‡, Valeriya A. Churumova‡, Natalya K. Tikhomirova‡, Pavel P. Philippov‡, and Karl-Wilhelm Koch§¶

From the ‡A. N. Belozersky Institute of Physico-Chemical Biology, M. V. Lomonosov Moscow State University, 119992 Moscow, Russia and §Institut für Biologische Informationsverarbeitung 1, Forschungszentrum Jülich, D-52425 Jülich, Germany

Cholesterol-rich membranes or detergent-resistant membranes (DRMs) have recently been isolated from bovine rod outer segments and were shown to contain several signaling proteins such as, for example, transducin and its effector, cGMP-phosphodiesterase PDE6. Here we report the presence of rhodopsin kinase and recoverin in DRMs that were isolated in either light or dark conditions at high and low Ca^{2+} concentrations. Inhibition of rhodopsin kinase activity by recoverin was more effective in DRMs than in the initial rod outer segment membranes. Furthermore, the Ca^{2+} sensitivity of rhodopsin kinase inhibition in DRMs was shifted to lower free Ca^{2+} concentration in comparison with the initial rod outer segment membranes (IC_{50} = 0.76 μM in DRMs and 1.91 μM in rod outer segments). We relate this effect to the high cholesterol content of DRMs because manipulating the cholesterol content of rod outer segment membranes by methyl-β-cyclodextrin yielded a similar shift of the Ca^{2+}-dependent dose-response curve of rhodopsin kinase inhibition. Furthermore, a high cholesterol content in the membranes also increased the ratio of the membrane-bound form of recoverin to its cytoplasmic free form. These data suggest that the Ca^{2+}-dependent feedback loop that involves recoverin is spatially heterogeneous in the rod cell.

Phototransduction in retinal rod and cone cells is started with the absorption of light by the photopigment rhodopsin, a seven-transmembrane helix receptor. Activated rhodopsin (metarhodopsin II) couples to a heterotrimeric G-protein, transducin, and thereby activates the visual enzymatic cascade that leads to the amplified hydrolysis of cGMP by cGMP-phosphodiesterase (1, 2). Cyclic nucleotide-gated cation channels in the photoreceptor plasma membrane are opened by cGMP in the dark and closed after hydrolysis of cGMP in light. Closure of channels causes hyperpolarization of the cell plasma membrane, which ultimately leads to a reduction of transmitter release at the synapse (3). A decrease in cytoplasmic cGMP is accompanied by a decrease in free cytoplasmic Ca^{2+}, which is sensed by Ca^{2+} sensor proteins that regulate their target proteins in a Ca^{2+}-dependent fashion. For example, calmodulin influences the ligand sensitivity of the cation channels (4), and guanylate cyclase-activating proteins activate two membrane-bound guanylate cyclases at low Ca^{2+} concentrations (5–9). Phosphorylation and deactivation of rhodopsin are catalyzed by rhodopsin kinase, which is under Ca^{2+}-dependent control by the Ca^{2+}-binding protein recoverin (10–13). These Ca^{2+}-dependent feedback loops are necessary to restore the dark state of the cell and to adjust the light sensitivity of the photoreceptor cell to different intensities of ambient illumination (1–3, 14).

A photoreceptor cell consists of distinct cellular compartments (outer segment, inner segment, and synaptic terminal), and these compartments differ in their Ca^{2+} homeostasis and protein content (1, 16). Protein translocation between compartments along the longitudinal axis was observed for some key signaling proteins such as transducin, arrestin, and protein phosphatase 2A (17–20). In addition, a spatial heterogeneity of the cholesterol content in the stacked disk membranes of rod outer segments (ROSs)[1] was observed along the axis of the outer segment. Newly formed disks at the basal part of the outer segment contain a high amount of cholesterol of ~30% of the total lipid content. The percentage of cholesterol decreases during aging of the disk membranes and reaches a mere 5% at the tip end of ROSs (21–23). Cholesterol can inhibit cGMP-phosphodiesterase activity (23) and interferes with formation of photoexcited rhodopsin by influencing membrane acyl chain packing (24). Taken together, these results point to a spatial heterogeneity of visual transduction in ROSs. In fact, single photon responses recorded from the tip of a toad ROS are smaller in amplitude and slower than responses recorded from the base. Background light reduces flash sensitivity at the tip more than at the base (25). Although this spatial heterogeneity of the light response has been known for more than 20 years, it has not been understood at the cellular and molecular levels.

Recent reports have stimulated discussion about the spatial heterogeneity of the rod light response. Detergent-resistant membranes (DRMs) or lipid rafts that contain a high cholesterol/phospholipid ratio have recently been isolated from bovine ROSs (26–30). A light-dependent translocation into DRMs has been demonstrated for transducin; its effector, cGMP-phos-

* This work was supported by grants from the Deutsche Forschungsgemeinschaft (to K.-W. K.); a grant from the Forschungszentrum Jülich for visiting scientists (to I. I. S. and P. P. P.); a grant from the Ludwig Institute for Cancer Research (to P. P. P.); a grant from the "International Projects" of the Ministry of Education and Science, Russian Federation (to P. P. P.); and Russian Foundation for Basic Research Grants 03-04-49181 (to P. P. P.) and 03-04-48909 (to I. I. S.) and INTAS (to I. I. S., P. P. P., and K.-W. K.). The costs of publication of this article were defrayed in part by the payment of page charges. This article must therefore be hereby marked "*advertisement*" in accordance with 18 U.S.C. Section 1734 solely to indicate this fact.

¶ To whom correspondence should be addressed: Institut für Biologische Informationsverarbeitung 1, Forschungszentrum Jülich, Postbox 1913, D-52425 Jülich, Germany. Tel.: 49-2461-61-3255; Fax: 49-2461-614216; E-mail: k.w.koch@fz-juelich.de.

[1] The abbreviations used are: ROS, rod outer segment; DRM, detergent-resistant membrane; PE, phosphatidylethanolamine; PC, phosphatidylcholine; HPLC, high pressure liquid chromatography; $[Ca^{2+}]_{free}$, free Ca^{2+} concentration.

phodiesterase; the shorter splice variant of arrestin p44; and the RGS9-Gβ5L complex (26, 27, 29, 30). ROM-1, a disk membrane protein, which probably functions as an adaptor protein, was copurified with DRM fractions but only showed a modest light-dependent distribution between the DRMs and the detergent-soluble fractions (28). Caveolin and membrane guanylate cyclase (probably retina-specific ROS-GC1) reside in DRMs but do not show any light-dependent translocation (26). Rod function is under dynamic control of Ca^{2+}-mediated feedback loops, and Ca^{2+} regulates the longitudinal transport of transducin (17), but it is not known whether any signaling proteins different from those mentioned above associate with DRMs or whether Ca^{2+} is involved in this association. In the present study, we investigated this issue as applied to the Ca^{2+} sensor recoverin and its target, rhodopsin kinase, to answer questions regarding whether these proteins associate with DRMs and which functional consequences follow from such an interaction.

EXPERIMENTAL PROCEDURES

Isolation of DRMs from Bovine Rod Outer Segments—ROSs from bovine retinae were purified according to a previously published procedure (15). DRMs or lipid rafts were isolated from bovine ROSs by the following procedure of Nair *et al.* (26), with some modifications. Briefly, ROSs were adjusted to ~10 mg/ml rhodopsin in buffer A (100 mM KCl, 2 mM $MgCl_2$, 1 mM dithiothreitol, and 10 mM Hepes, pH 7.4). For one gradient, 500 μl of ROSs in buffer A were mixed with 2 ml of buffer B (12.5 mM Tris, pH 7.4, 1.25 mM $CaCl_2$, 1.25 mM $MgCl_2$, and 0.63% (v/v) Triton X-100) and incubated for 5 min on ice or at 4 °C. This solution was mixed with 2.5 ml of 80% (w/v) sucrose in an ultracentrifuge tube. The mixture was then carefully overlaid with 4.6 ml of 30% sucrose and 2.3 ml of 5% sucrose. Samples were centrifuged at 24,000 rpm in SW-41 rotor (Beckman) at 4 °C overnight. The whole procedure was performed in either dim red light (dark) or under daylight conditions. In some preparations, $CaCl_2$ was replaced by 1 mM EGTA. When gradients were run for comparison, exactly the same amount of ROS was loaded on the gradient. In addition, we increased the Triton X-100 concentration that was used for solubilization to 1% and 2% (v/v). Alternatively, we isolated DRMs according to the procedure of Boesze-Battaglia *et al.* (28). After centrifugation, we collected ~24 fractions (500 μl) of the gradient from bottom to the top using a glass capillary tube and a perstaltic pump.

Determination of Rhodopsin and Cholesterol—Rhodopsin concentration in purified ROSs or in fractions obtained after DRM isolation and fractionation was determined spectrophotometrically at 498 nm using a molar extinction coefficient of 40,000 $M^{-1} \times cm^{-1}$. The amount of rhodopsin (in mg) in each of the 25 fractions was summed up and set as 100%. Numbering starts with fractions at the top. Cholesterol was determined by a diagnostic kit according to the manufacturer's protocol (Sigma and Rolf Greiner Biochemica, Flacht, Germany). The principle of the assay is as follows: cholesterol is oxidized to cholest-4-en-3-one and H_2O_2 by cholesterol oxidase. H_2O_2 was allowed to react with hydroxybenzoic acid and 4-aminoantipyrin in the presence of peroxidase to yield chinomeimin, a dye that can be measured spectrophotometrically at 530 nm.

Adjusting Cholesterol in ROS Membranes—The cholesterol exchange between methyl-β-cyclodextrin and ROSs was performed as described previously (24). Briefly, urea-washed ROS membranes (30 μM rhodopsin) in 10 mM Tris-HCl (pH 7.5), 60 mM NaCl, and 30 mM KCl were incubated with methyl-β-cyclodextrin in the presence or absence of 2 mM cholesterol. Mixtures were incubated in the dark at 25 °C for 2 h. Afterward, ROS membranes were pelleted by centrifugation for 30 min at 29,000 $\times$ *g*. The pellet was resuspended in 10 mM Tris-HCl (pH 7.5) containing 0.1 mM EDTA and 5% (w/v) Ficoll. Aliquots of this suspension were layered on top of 31% sucrose in 10 mM Tris-HCl (pH 7.5) and overlaid with 10 mM Tris-HCl (pH 7.5). Tubes were spun for 3 h at 21,000 rpm in a Beckman SW-28 rotor. Layers with ROS membranes were collected with a syringe and washed three times with 10 mM Tris-HCl (pH 7.5). The cholesterol content of each sample was measured by using the Amplex red kit (Molecular Probes), according to the manufacturer's directions. Cholesterol content is expressed as a percentage (w/w) of phospholipids. Phospholipid content was determined as follows. Lipids were extracted from ROS membrane suspensions by chloroform-methanol (2:1, v/v) and by a second extraction step using chloroform-methanol-HCl (200:100:1, v/v). Further processing of the lipid-containing fractions was as described previously (31). Phospholipids in the lipid extract from ROS membranes were analyzed by normal phase HPLC (silica gel cartridge, 0.46 $\times$ 20 cm; Vydac) essentially as described previously (32–34), using the UV absorption between 200 and 210 nm for detection. Known standards of phospholipids were injected into the HPLC to quantitate the unknown phospholipid content of ROS membranes.

Purification of Recoverin and Phosphorylation of Rhodopsin—Myristoylated recoverin was heterologously expressed in *Escherichia coli* and purified from a cell extract as described previously (35, 36). Phosphorylation of rhodopsin was assayed as described in Ref. 35 at 25 °C in the reaction mixture (50 μl) containing 20 mM Tris-HCl (pH 7.5), 150 mM NaCl, 3 mM $MgCl_2$, 200 μM [γ-^{32}P]ATP (1–3 $\times$ 10^5 cpm/nmol), about 1 unit of rhodopsin kinase, ROS membranes or DRMs (see figure legends), and myristoylated recoverin (see figure legends). Free calcium concentration ($[Ca^{2+}]_{free}$) was adjusted as described previously (35) and varied as indicated in the corresponding figures. Immediately after illumination of the mixture (100% bleaching of rhodopsin), ATP was added to start the reaction, which was stopped 20 min later or by the addition of the 2× SDS-PAGE sample buffer. After SDS-PAGE of the samples, zones of rhodopsin were cut out, and ^{32}P incorporation was estimated by Cherenkov counting.

Surface Plasmon Resonance Spectroscopy—Hydrophobic L1 sensor chips (Biacore, Stockholm, Sweden) were used to immobilize lipid mixtures of phosphatidylcholine, phosphatidylethanolamine, and cholesterol. Recoverin was applied in the mobile phase in running buffer (10 mM Hepes, pH 7.5, 150 mM KCl, 20 mM $MgCl_2$, and 0.2 mM $CaCl_2$) at a flow rate at 5 μl/min. Details of surface plasmon resonance experiments and analysis have been described elsewhere (35–37).

Other Methods—Equilibrium centrifugation assay for the binding of recoverin to liposomes, SDS-PAGE, and Western blotting have been described previously (8, 35). Antibodies for Western blotting were from the following sources and used at indicated dilutions: polyclonal anti-recoverin (Ref. 38; 1:10,000) and polyclonal anti-ROS-GC1 (Ref. 39, 1:1,000). Polyclonal anti-rhodopsin kinase (1:1,000), polyclonal anti-transducin α (1:1,000), and polyclonal anti-caveolin (1:200) were from Santa Cruz Biotechnology (Santa Cruz, CA).

RESULTS

We isolated a Triton X-100-insoluble membrane fraction from bovine ROS using a sucrose density gradient centrifugation. Samples were fractionated after the centrifugation step, and the cholesterol content along the gradient was determined by a colorimetric assay. Almost all cholesterol was found in a peak that centered around fraction 6 (Fig. 1*A*). This distribution pattern of cholesterol was not changed significantly when we performed the whole isolation procedure either in the presence of Ca^{2+} or EGTA, after illumination, or in the dark (Fig. 1*A*). The main cholesterol peak coincided with the position of a nearly transparent yellow band at the boundary between 5% and 30% sucrose. This band (boundary fraction) has previously been identified as DRMs or lipid rafts from ROS (26–28).

The rhodopsin distribution along the sucrose gradient was analyzed by absorption measurements. The main portion of rhodopsin was solubilized by Triton X-100 and found in fractions 12–23 (89%); a smaller portion of ~10% was found at the 5% and 30% sucrose boundary (fractions 5–9) and comigrated with the cholesterol peak (Fig. 1*B*). Up to 23% rhodopsin was found in DRMs. Fractions 1 and 2 contained only 1% rhodopsin. The presence of rhodopsin in DRMs is consistent with previous observations (27). A critical parameter for solubilization of rhodopsin was the rhodopsin/Triton X-100 ratio. For example, when we treated ROSs containing 4.5–4.6 mg/ml rhodopsin with 0.5% or 1% (v/v) Triton X-100, the amount of rhodopsin and other proteins in DRMs was similar at both detergent concentrations. However, decreasing the start amount of rhodopsin to 1.7 mg/ml in either 1% or 2% Triton X-100 led to almost complete solubilization of rhodopsin (<1% rhodopsin in DRMs). The cholesterol peak at the boundary between 5% and 30% sucrose also decreased by increasing Triton X-100: whereas at 0.5% Triton X-100, nearly 100% of total cholesterol comigrated with the boundary fraction, it was 37% and 12% of

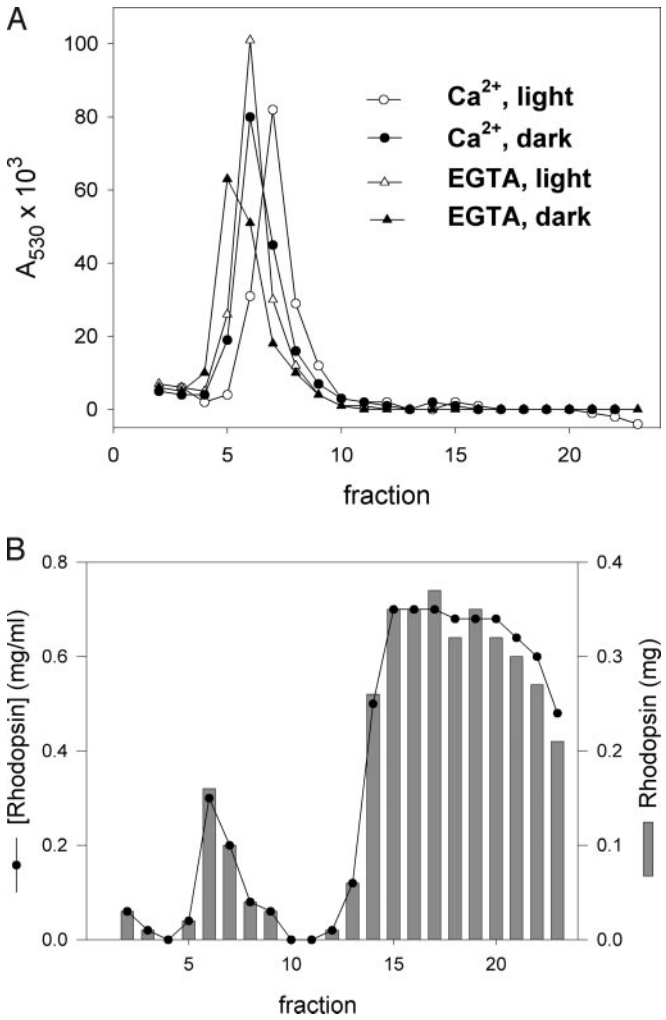

FIG. 1. **Distribution of cholesterol (*A*) and rhodopsin (*B*) along a sucrose gradient.** Fractions of ~0.5 ml were collected and measured for content of cholesterol (absorbance at 530 nm in *A*) and rhodopsin (*B*). Numbering of fractions goes from top (fraction 1) to bottom (fraction 23). Fractions 4–9 contain DRMs. Preparations were performed with or without Ca^{2+} in the dark or after illumination as indicated in *A*. Rhodopsin concentration was determined in the dark-kept fractions (gradient run in the presence of Ca^{2+}) and expressed in mg/ml. *Gray bars* in *B* indicate the total amount (mg) of rhodopsin in each fraction.

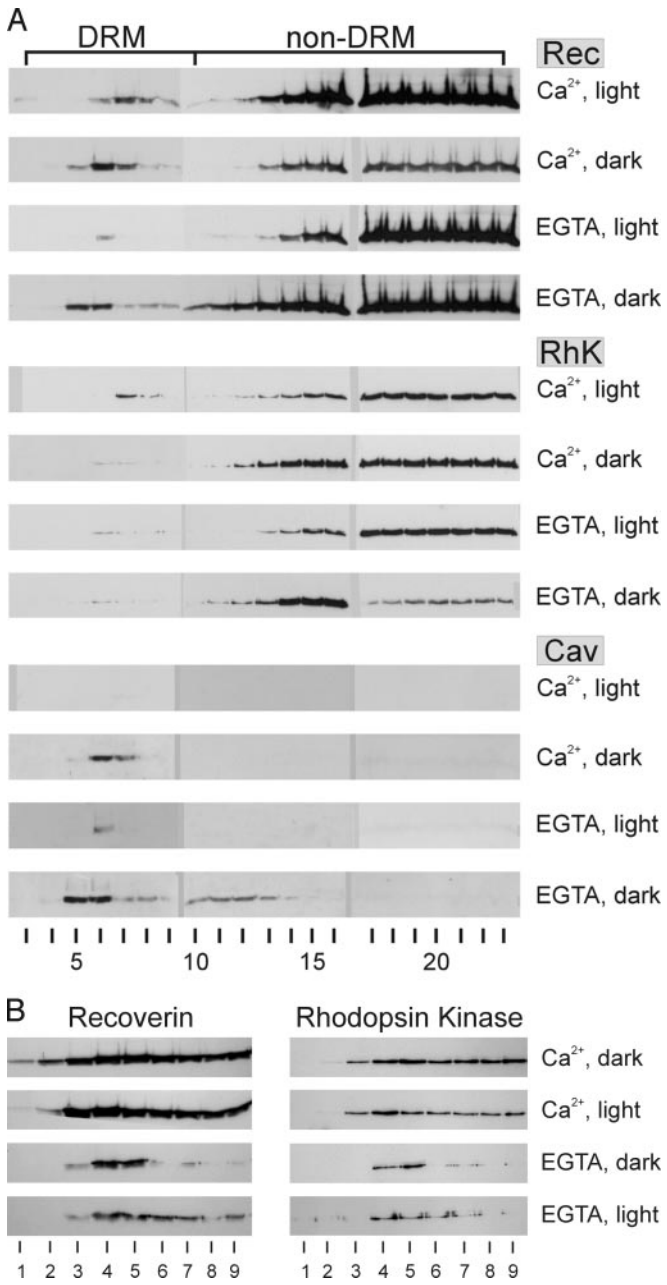

FIG. 2. **Distribution of recoverin and rhodopsin kinase in DRMs and non-DRMs obtained under different conditions.** *A*, 42 μl of each of the fractions (fractions 3–23) shown in Fig. 1 was loaded on a SDS-polyacrylamide gel and analyzed. Proteins (recoverin, rhodopsin kinase, and caveolin-1) were detected by Western blotting. Conditions under which the sucrose gradients were run are indicated. *B*, distribution of recoverin and rhodopsin kinase in DRMs of different gradient runs under the indicated conditions. The starting concentration of rhodopsin was 1.84 mg/ml instead of 1.66 mg/ml, and therefore the rhodopsin:Triton X-100 ratio was slightly higher than that in *A*.

total cholesterol at 1% Triton X-100 and 2% Triton X-100, respectively. These results showed that rhodopsin was completely solubilized under conditions that left a significant amount of cholesterol associated with the boundary fraction.

We further tested by Western blotting whether other ROS membrane proteins known to be associated with DRMs (26–30) are present in our DRM preparation. Guanylate cyclase ROS-GC1 and cGMP-phosphodiesterase were present in DRM and non-DRM fractions; transducin showed a clear light-dependent translocation into the DRM fraction (data not shown). Caveolin, a marker protein for lipid rafts, was found almost exclusively in the DRM fraction (Fig. 2*A*). Interestingly, less caveolin was detected in DRMs after illumination (Fig. 2*A*). Although the intensity of caveolin staining was variable, we observed this light-dependent distribution of caveolin in two independent fractionation studies. It is known that caveolin associates in a cholesterol-dependent manner with transducin (29) and that transducin undergoes a light-dependent translocation from the outer segment to the inner segment (17, 18). A combination of these two effects could explain our observation.

In summary, we conclude from these results that our DRM preparation from bovine ROS contains the same signaling proteins as reported by other investigators. It is therefore suitable for our further investigations.

When we probed all fractions of the gradient by antibodies against recoverin and rhodopsin kinase, both proteins were detected in the DRM and non-DRM fraction. A comparison of the gradients run in the presence of Ca^{2+} or EGTA under dark or light conditions showed in all cases the presence of recoverin and rhodopsin kinase in the DRM fraction and a clear segregation between DRM and non-DRM fractions (Fig. 2*A*). However, the relative amount of each protein in DRMs was influenced by Ca/EGTA and/or by illumination. For example,

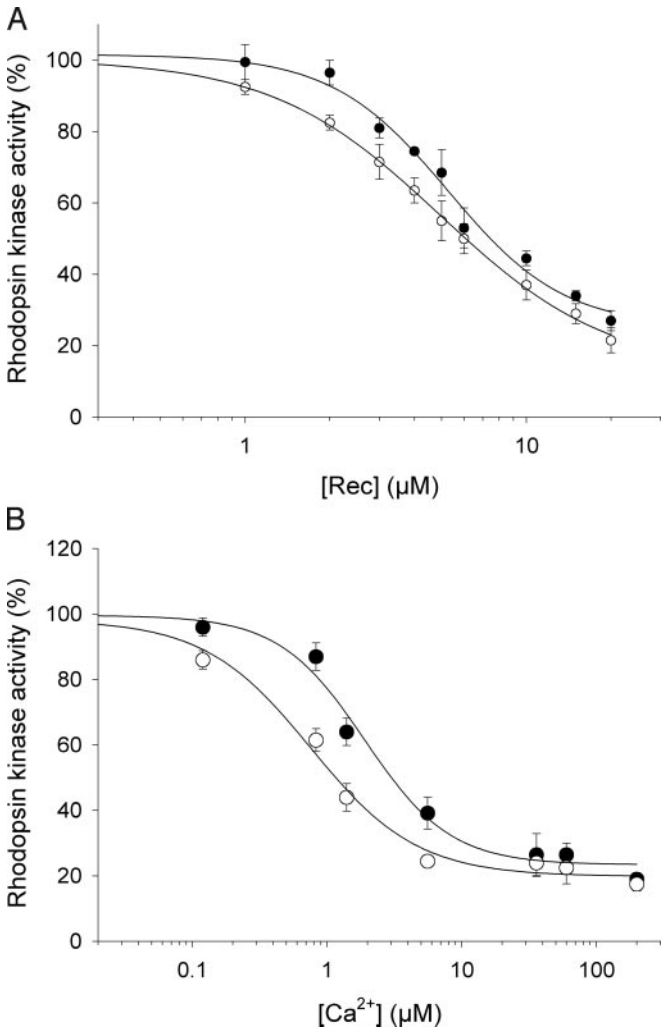

FIG. 3. **Rhodopsin kinase activity in isolated DRMs was compared with the activity in ROS membranes.** *A*, Pelleted DRMs (○) or ROS membranes (●) were incubated with rhodopsin kinase at 200 μM $CaCl_2$ and increasing concentrations of recoverin. Inhibition was half-maximal at 5.3 μM recoverin with ROS membranes and 4.9 μM recoverin with DRMs. *B*, Pelleted DRMs (○) or ROS membranes (●) were incubated with 20 μM recoverin and rhodopsin kinase at different $[Ca^{2+}]_{free}$. IC_{50} values for Ca^{2+} were 1.91 μM (ROS membranes) and 0.76 μM (DRMs). DRMs were prepared in the absence of Ca^{2+} after illumination; they contained only a small amount of endogenous rhodopsin kinase and recoverin.

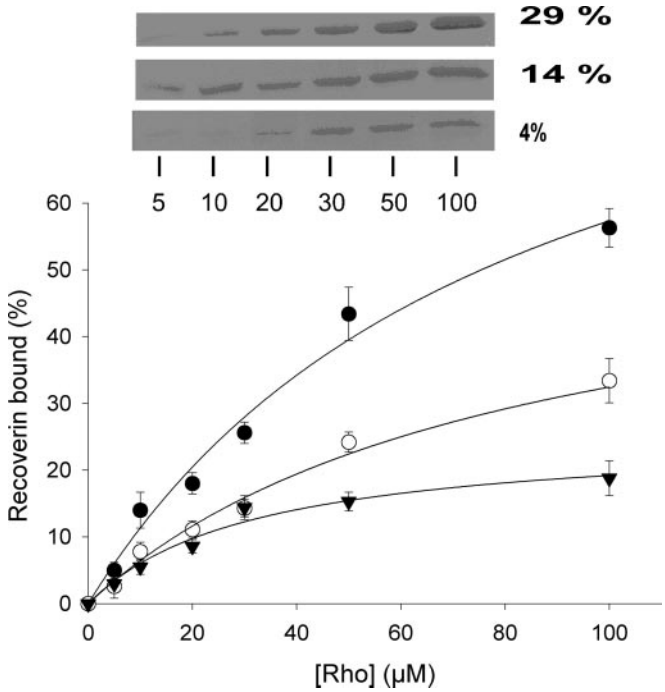

FIG. 4. **Binding of recoverin to native ROS membranes with different percentages of cholesterol.** Cholesterol in native ROS membranes was adjusted by treatment with methyl-β-cyclodextrin (●, 29.6%; ○, 14%; ▼, 4.1% cholesterol). Recoverin (30 μM) was incubated with membranes at different rhodopsin concentrations and analyzed by equlibrium centrifugation assay. *Inset*, corresponding SDS-PAGE analysis (Coomassie Blue staining) of membrane-bound recoverin at different percentages of cholesterol (*right*) and the indicated rhodopsin concentration (*bottom*).

recoverin in the DRM fraction decreased after illumination in the presence of EGTA (Fig. 2*A*). Distribution of rhodopsin kinase resembled that of recoverin, but the presence of rhodopsin kinase became most prominent after illumination in the presence of Ca^{2+}. The relative amount of recoverin and rhodopsin kinase in DRMs varied among different preparations, as can be seen best in a comparison of Fig. 2*A* with Fig. 2*B*. The effect of switching from Ca^{2+} to EGTA during DRM isolation is more pronounced in Fig. 2*B* because the presence of EGTA reduced the amount of recoverin and rhodopsin kinase in the DRM fraction.

We next asked whether the inhibition of rhodopsin kinase activity by recoverin in DRMs differs from the inhibition in ROS membranes. In titration experiments, we varied either the recoverin concentration at saturating $[Ca^{2+}]$ or $[Ca^{2+}]_{free}$ at a constant recoverin concentration. At saturating $[Ca^{2+}]$, inhibition of rhodopsin kinase occurred at slightly lower recoverin concentrations (Fig. 3*A*). However, when we compared the Ca^{2+}-dependent phosphorylation of rhodopsin in ROS membranes with that in isolated DRMs, we observed a significant shift of the IC_{50} to lower free Ca^{2+} concentrations (from 1.91 μM in ROS membranes to 0.76 μM in DRMs) (Fig. 3*B*). Thus, recoverin was more effective as an inhibitor of rhodopsin kinase in DRMs than it was in ROS membranes. Overall activity of rhodopsin kinase without interference by recoverin was identical in ROS membranes and DRMs for nearly 20 min of incubation. Longer incubation times showed ~20% lower kinase activity in ROS membranes.

Because cholesterol is a main constituent of DRMs, we tested how cholesterol influenced the membrane association and inhibitory properties of recoverin. The cholesterol content of native bovine ROS membranes was manipulated by treatment with methyl-β-cyclodextrin, and the binding of recoverin was measured by a centrifugation equilibrium assay. Native ROS membranes contained, on average, 14% cholesterol. Decreasing the cholesterol content to 4.1% also decreased the amount of bound recoverin, whereas an increase of cholesterol to 29.6% increased the amount of bound recoverin at least 2-fold (Fig. 4). These results showed that binding of recoverin to membranes strongly depended on the cholesterol content of the membranes. Control incubations with nonmyristoylated recoverin and arrestin showed no dependence on either Ca^{2+}/EGTA or the percentage of cholesterol (data not shown).

We also tested the recoverin-dependent inhibition of rhodopsin kinase activity when cholesterol in ROS membranes was varied (Fig. 5*A*). The kinase activity was determined by measuring phosphorylation of rhodopsin. Inhibition of rhodopsin kinase was half-maximal at 6.6 μM recoverin in untreated ROS (14% cholesterol) and shifted to a higher value when cholesterol was lowered (IC_{50} = 10.4 μM at 4.1% cholesterol) or to a lower value when cholesterol was higher (IC_{50} = 4.5 μM at 29.6% cholesterol).

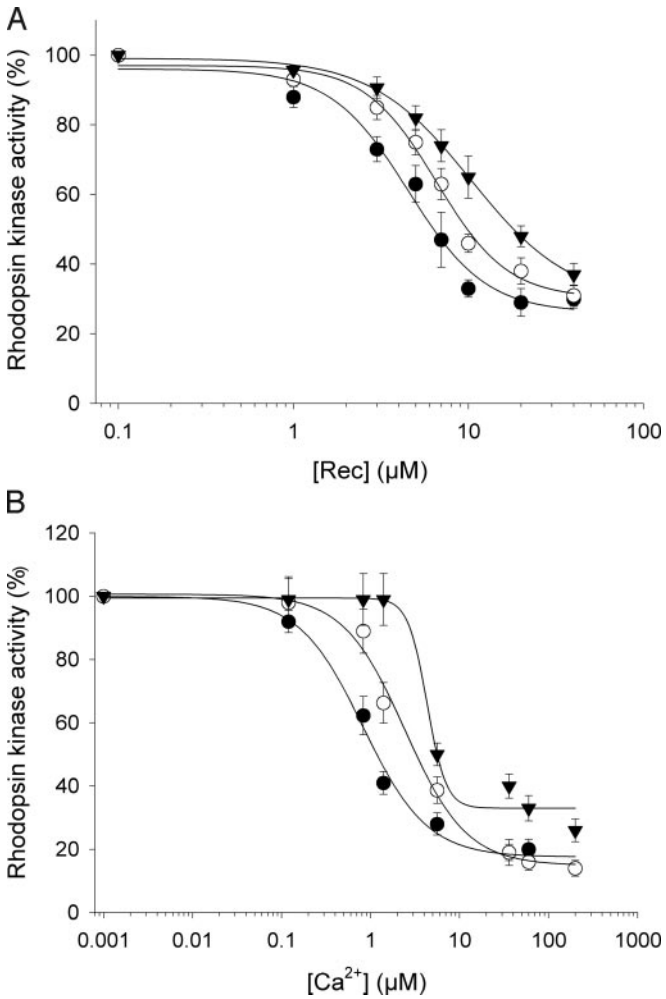

FIG. 5. **Rhodopsin kinase activity at different cholesterol levels.** *A*, Rhodopsin kinase activity was determined as a function of recoverin concentration. Different cholesterol levels in membranes were adjusted by treatment with methyl-β-cyclodextrin (●, 29.6%; ○, 14%; ▼, 4.1%). Half-maximal inhibition was at 4.5, 6.6, and 10.4 μM recoverin at 29.6%, 14%, and 4.1% cholesterol, respectively. *B*, Rhodopsin kinase activity was measured as a function of $[Ca^{2+}]_{free}$ in the presence of 20 μM recoverin. Cholesterol adjustment and symbols are the same as those described in *A*. IC_{50} values of $[Ca^{2+}]_{free}$ were 0.82 (29.6% cholesterol), 2.43 (14% cholesterol), and 4.31 μM (4.1% cholesterol).

Inhibition of rhodopsin kinase by recoverin depends also on $[Ca^{2+}]_{free}$ (11–13). We tested whether a change in the cholesterol content of native ROS membranes has any influence on the Ca^{2+}-dependent activity of rhodopsin kinase. Increasing the cholesterol content from 4.1% to 29.4% shifted the dose-response curve to lower $[Ca^{2+}]_{free}$, and the IC_{50} changed from 4.31 to 0.82 μM $[Ca^{2+}]_{free}$ (Fig. 5*B*). At intermediate levels of cholesterol, the IC_{50} was 2.43 μM. These results were consistent with our observation that inhibition of rhodopsin kinase by recoverin is more efficient and occurs at lower $[Ca^{2+}]_{free}$ in DRMs than in ROS membranes. The results also implicate that the shift in the dose-response curve shown in Fig. 3 cannot be attributed to detergent treatment because no detergents were needed to adjust different cholesterol levels. Furthermore, the binding experiments shown in Fig. 4 indicate that recoverin is bound more strongly to membranes when higher cholesterol levels are adjusted.

We also tested the influence of cholesterol on the membrane association of recoverin at saturating $[Ca^{2+}]$ using phospholipid vesicles containing phosphatidylethanolamine (PE) and phosphatidylcholine (PC) at a ratio of 50:50 without cholesterol or with increasing amounts of cholesterol (5–50%) by keeping

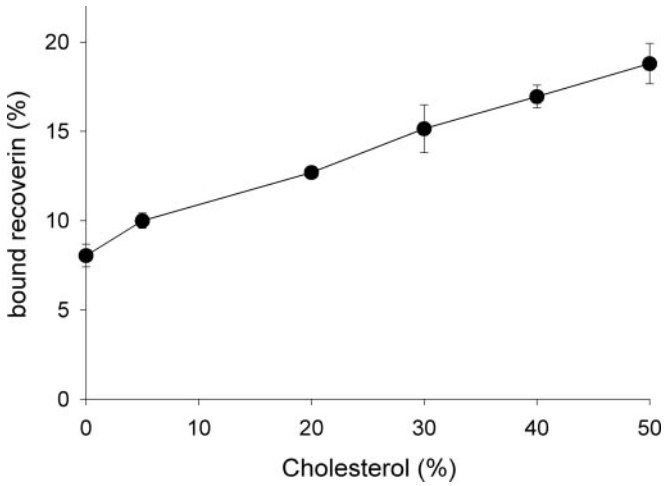

FIG. 6. **Binding of recoverin to liposomes as a function of cholesterol.** Liposomes with varying cholesterol content were incubated with 20 μM recoverin in the presence of 200 μM $CaCl_2$. After centrifugation, the amount of bound recoverin was determined.

the PC:PE ratio constant. Binding of recoverin to the vesicles was tested by an equilibrium centrifugation assay. Vesicles without cholesterol showed less than half of recoverin binding compared with vesicles containing increasing amounts of cholesterol in addition to PE and PC (Fig. 6).

In our previous work, we used immobilized lipids on sensor chips to explore membrane association of recoverin by surface plasmon resonance spectroscopy (35–37). Here we applied this method to test the influence of cholesterol upon recoverin binding to immobilized lipids. A phospholipid mixture of PE and PC (50:50) was immobilized on a hydrophobic sensor chip, and association of myristoylated recoverin was recorded in the presence of saturating $[Ca^{2+}]$. The resonance signal exhibited a rapid association phase and a biphasic dissociation phase that is typical for wild-type myristoylated recoverin (Fig. 7*A*; compare with Fig. 5 in Ref. 35). When the immobilized lipid mixture contained cholesterol (Fig. 7*A*, *top trace*), the maximal amplitude of the binding signal increased about 2-fold. Interestingly, the slower phase of the biphasic dissociation signal was more prominent in the presence of cholesterol. Variation of the recoverin concentration revealed the same result: in the presence of cholesterol, the maximal amplitude of the binding signal was at least twice as high as that in the absence of cholesterol (Fig. 7*B*). Control recordings with protein G in the presence and absence of cholesterol showed no significant difference of sensorgram amplitudes, which were similar to the amplitude we reported previously for protein G binding to an immobilized lipid mix (see Fig. 3*B* in Ref. 35).

In summary, our results suggest that the high cholesterol content of DRMs facilitates binding of recoverin to membranes and enforces inhibition of rhodopsin kinase by two means: it decreases the amount of recoverin at which kinase activity is half-maximal, and it shifts the dose-response curve to lower $[Ca^{2+}]_{free}$.

DISCUSSION

The light-driven transport of signaling proteins between photoreceptor cell compartments has received growing attention in recent years (17–20). In addition to these longitudinal transport processes, lateral translocation of proteins within disk membranes and into DRMs or lipid rafts has come into focus (26–30). Here we show for the first time that the Ca^{2+} sensor recoverin and its target, rhodopsin kinase, are present in DRMs of bovine rod cells and undergo a Ca^{2+}-dependent translocation within ROS membranes. A decrease of Ca^{2+}, by

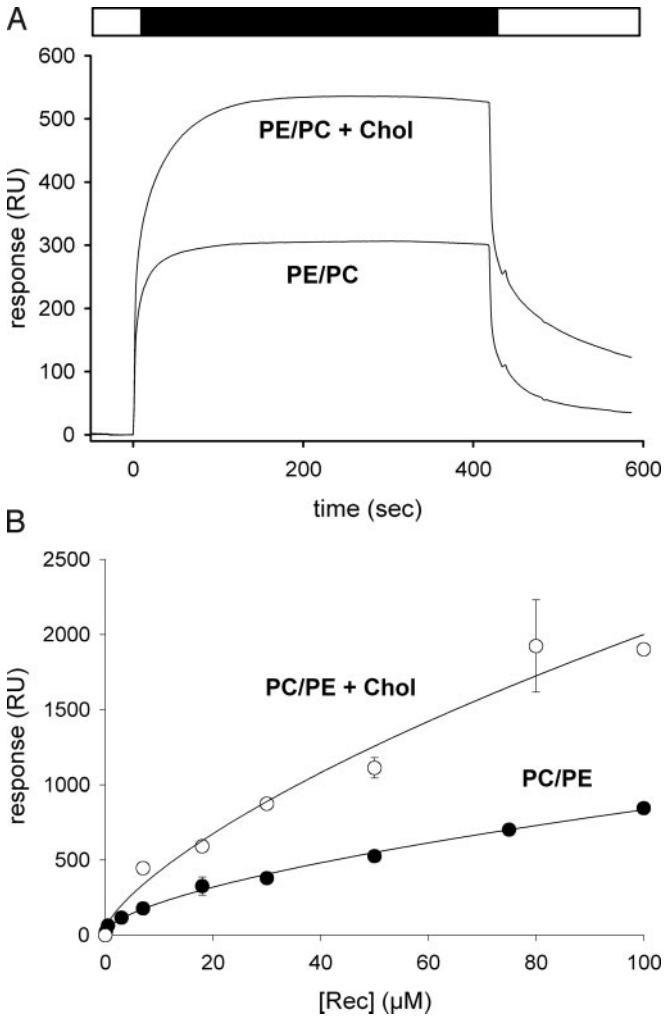

FIG. 7. **Surface plasmon resonance analysis of recoverin binding to immobilized lipids.** *A*, Lipids containing PE:PC at a ratio of 50:50 or PE:PC:cholesterol at a ratio of 25:25:50 were immobilized on a hydrophobic L1 sensor chip. Recoverin (5 μM) was injected into the buffer flow over the surface (*black bar*). Sensorgrams were run in the presence of 200 μM $CaCl_2$. *B*. Maximal amplitudes of recorded sensorgrams were plotted as a function of the injected recoverin concentration. Two different lipid layers were compared as described in *A*.

complexing with EGTA, minimized the presence of recoverin and rhodopsin kinase in DRMs. This finding reflects the Ca^{2+}-myristoyl switch of recoverin (40) and also the Ca^{2+}-dependent interaction of recoverin with rhodopsin kinase (10–13). Recoverin has a myristoyl group covalently attached at its N terminus. In the presence of Ca^{2+}, this group is exposed and facilitates membrane binding. Decreasing Ca^{2+} leads to a conformational change that enables the myristoyl group to be buried inside a hydrophobic pocket of the protein. As a consequence, recoverin is released from the membrane (40). Our data show that the driving force of recoverin to associate with DRMs was the high cholesterol content that is a characteristic property of DRMs preparations.

According to our present data, cholesterol has a profound effect on the efficiency with which recoverin controls rhodopsin kinase activity. In cholesterol-containing DRMs, inhibition of rhodopsin kinase became more efficient at lower $[Ca^{2+}]_{free}$. There has been a dispute in the literature (13, 41–43) about the physiological role of rhodopsin kinase inhibition by recoverin, but recent work on recoverin knockout mice has shown that the physiological role of recoverin is consistent with an effective prolongation of the catalytic activity of photoexcited rhodopsin (*i.e.* inhibition of rhodopsin kinase; Ref. 44). A main argument against such a role under *in vivo* conditions is the experimentally observed high IC_{50} for $[Ca^{2+}]_{free}$, which is about 1 order of magnitude higher than the cytoplasmic $[Ca^{2+}]_{free}$ in a dark-adapted rod cell (41). However, it has been argued that the IC_{50} value can be shifted into the physiologically relevant range when the data on rhodopsin kinase inhibition are extrapolated to the membrane-rich *in vivo* conditions of the rod cell (13, 42). Our results may provide an experimentally based solution to this problem because we show that high cholesterol content in membranes can shift the IC_{50} to lower $[Ca^{2+}]_{free}$: 0.76 μM in native DRMs and 0.82 μM in ROS membranes with high cholesterol content (29.6%). These values are in the physiological range of free Ca^{2+} in rod cells. Our data also show that the ratio of membrane-bound recoverin to cytoplasmic free recoverin is increased at high cholesterol content (Fig. 4), which causes more effective inhibitory action of recoverin.

In accordance with the well-described cholesterol gradient in rods (5% at the tip and 30% at the base; see "Introduction"), one could conclude that control of rhodopsin kinase activity by recoverin is spatially heterogenous and thus would contribute to the shape of the photoresponse at the base of a ROS differently than at the tip. It is known that photoresponses from rods depend on the longitudinal position of photon absorption (25). Responses from the base of a ROS are faster and have a larger peak amplitude; in the presence of background light flash, sensitivity is lower at the tip than at the base of ROS. If inhibition of rhodopsin kinase is stronger at the base than at the tip, the photoresponse of a dark-adapted cell would become larger and last longer. However, this is opposite to what was observed after single photon absorption (25). However, flash sensitivity in the presence of background light is higher at the base of the ROS, which would be consistent with a stronger inhibition of rhodopsin kinase at the base.

The above prediction is rather simplified and made under the assumption that other proteins have similar properties in DRMs and outside DRMs. However, Tα is suggested to have a reduced coupling to rhodopsin in DRMs (26). Furthermore, cholesterol inhibits cGMP-phosphodiesterase activity and metarhodopsin II formation (23, 24); cholesterol inhibits the latter by influencing the acyl chain packing of surrounding lipids. Finally, the splice variant of arrestin p44 that is found in DRMs after illumination (26) can be bound to nonphosphorylated metarhodopsin II with a rather low off-rate (0.07 s^{-1}) and would thereby prevent transducin activation (45). Together, these findings suggest that phototransduction in DRMs is less efficient.

A significant amount of rhodopsin (10–23% of total) was also found in DRMs, but increasing the Triton X-100 concentration led to the complete solubilization of rhodopsin, whereas a significant amount of cholesterol still comigrated with the 5%/30% boundary. These results could indicate that rhodopsin is not associated with DRMs or simply that Triton X-100 has a higher potency to solubilize rhodopsin than to solubilize cholesterol. We cannot distinguish between these possibilities. Furthermore, our data do not allow us to draw any conclusions about the preexistence of rafts before treatment with detergent. However, we emphasize that the existence or nonexistence of rafts is irrelevant to our observation that cholesterol has a significant impact on membrane association of recoverin and on inhibition of rhodopsin kinase. Thus, taking the cholesterol gradient in ROSs into account, we assume that rhodopsin in a cholesterol rich-environment is more restricted in diffusion and that phototransduction in DRMs works less efficiently (see above for a discussion of the literature). As a consequence, the base of the ROS would contain a significant amount of signaling proteins in a "caged-like state" unable to transmit the light

signal. This reduction in signaling molecules is reminiscent of transgenic mice that harbor a hemizygous knockout of rhodopsin resulting in a reduction of rhodopsin by 50% (46). Photoresponses from these transgenic mice have accelerated rising and recovery phases due to less protein crowding and facilitated diffusion. In fact, they qualitatively resemble the single photon responses from ROS base with faster rising and recovery phases.

In summary, inhibition of rhodopsin kinase by recoverin (*i.e.* less efficient phosphorylation of rhodopsin) seems to be more pronounced at the base than at the tip of ROS, if we consider the effects of different cholesterol contents. Interpretation of photoresponses published in the literature leads us to suggest that these signaling events are more important under constant background light and not under the single photon regime of dark-adapted rods.

REFERENCES

1. Pugh, E. N., Jr., and Lamb, T. D. (2000) in *Handbook of Biological Physics* (Stavenga, D. G., DeGrip, W. J., and Pugh, E. N., Jr., eds) pp. 183–255, Elsevier Science B.V. (North Holland), Amsterdam
2. Burns, M. E., and Baylor, D. A. (2001) *Annu. Rev. Neurosci.* **24,** 779–805
3. Kaupp, U. B., and Seifert, R. (2002) *Physiol. Rev.* **82,** 769–824
4. Hsu, Y.-T., and Molday, R. S. (1993) *Nature* **361,** 76–79
5. Palczewski, K., Subbaraya, I., Gorczyca, W. A., Helekar, B. S., Ruiz, C. C., Ohguro, H., Huang, J., Zhao, X., Crabb, J. W., Johnson, R. S., Walsh, K. A., Gray-Keller, M. P., Detwiler, P. B., and Baehr, W. (1994) *Neuron* **13,** 395–404
6. Dizhoor, A. M., Olshevskaya, E. V., Henzel, W. J., Wong, S. C., Stults, J. T., Ankoudinova, I., and Hurley, J. B. (1995) *J. Biol. Chem.* **270,** 25200–25206
7. Gorczyca, W. A., Polans, A. S., Surgucheva, I. G., Subbaraya, I., Baehr, W., and Palczewski, K. (1995) *J. Biol. Chem.* **270,** 22029–22036
8. Frins, S., Bönigk, W., Müller, F., Kellner, R., and Koch, K.-W. (1996) *J. Biol. Chem.* **271,** 8022–8027
9. Haeseleer, F., Sokal, I., Li, N., Pettenati, M., Rao, N., Bronson, D., Wechter, R., Baehr, W., and Palczewski, K. (1999) *J. Biol. Chem.* **274,** 6526–6535
10. Kawamura, S., Hisatomi, O., Kayada, S., Tokunaga, F., and Kuo, C.-H. (1993) *J. Biol. Chem.* **268,** 14579–14582
11. Gorodovikova, E. N., Gimelbrant, A. A., Senin, I. I., and Philippov, P. P. (1994) *FEBS Lett.* **349,** 187–190
12. Chen, C.-K., Inglese, J., Lefkowitz, R. J., and Hurley, J. B. (1995) *J. Biol. Chem.* **270,** 18060–18066
13. Klenchin, V. A., Calvert, P. D., and Bownds, M. D. (1995) *J. Biol. Chem.* **270,** 16147–16152
14. Pugh, E. N., Jr., Nikonov, S., and Lamb, T. D. (1999) *Curr. Opin. Neurobiol.* **9,** 410–418
15. Koch, K.-W., Lambrecht, H.-G., Haberecht, M., Redburn, D., and Schmidt, H. H. H. W. (1994) *EMBO J.* **13,** 3312–3320
16. Krizaj, D., and Copenhagen, D. R. (1998) *Neuron* **21,** 249–256
17. Pulvermüller, A., Giessl, A., Heck, M., Wottrich, R., Schmitt, A., Ernst, O. P., Choe, H.-W., Hofmann, K. P., and Wolfrum, U. (2002) *Mol. Cell. Biol.* **22,** 2194–2203
18. Sokolov, M., Lyubarsky, A. L., Strissel, K. J., Savchenko, A. B., Govardovskii, V. I., Pugh, E. N., Jr., and Arshavsky, V. Y. (2002) *Neuron* **33,** 95–106
19. Zhang, H., Huang, W., Zhu, X., Craft, C. M., Baehr, W., and Chen, C.-K. (2003) *Mol. Vis.* **9,** 231–237
20. Brown, B. M., Carlson, B. L., Zhu, X., Lolley, R. N., and Craft, C. M. (2002) *Biochemistry* **41,** 13526–13538
21. Boesze-Battaglia, K., Hennessey, T., and Albert, A. D. (1989) *J. Biol. Chem.* **264,** 8151–8155
22. Boesze-Battaglia, K., Fliesler, S. J., and Albert, A. D. (1990) *J. Biol. Chem.* **265,** 18867–18870
23. Boesze-Battaglia, K., and Albert, A. D. (1990) *J. Biol. Chem.* **265,** 20727–20730
24. Niu, S.-L., Mitchell, D. C., and Litman, B. J. (2002) *J. Biol. Chem.* **277,** 20139–20145
25. Schnapf, J. L. (1983) *J. Physiol.* (*Lond.*) **343,** 147–159
26. Nair, K. S., Balasubramanian, N., and Slepak, V. Z. (2002) *Curr. Biol.* **12,** 421–425
27. Seno, K., Kishimoto, M., Abe, M., Higuchi, Y., Mieda, M., Owada, Y., Yoshiyama, W., Liu, H., and Hayashi, F. (2001) *J. Biol. Chem.* **276,** 20813–20816
28. Boesze-Battaglia, K., Dispoto, J., and Kahoe, M. A. (2002) *J. Biol. Chem.* **277,** 41843–41849
29. Elliott, M. H., Fliesler, S. J., and Ghalayini, A. J. (2003) *Biochemistry* **42,** 7892–7903
30. Liu, H., Seno, K., and Hayashi, F. (2003) *Biochem. Biophys. Res. Commun.* **303,** 19–23
31. Wuthier, J. (1996) *J. Lipid Res.* **7,** 558–561
32. Hurst, W. J., and Martin, R. A. (1984) *J. Am. Oil Chem. Soc.* **61,** 1462–1463
33. Letter, W. S. (1992) *J. Liquid Chromatogr.* **15,** 253–266
34. Brouwers, J. F. H. M., Gadella, B. M., van Godde, L. M. G., and Tielens, A. G. M. (1998) *J. Lipid Res.* **39,** 344–353
35. Senin, I. I., Fischer, T., Komolov, K. E., Zinchenko, D. V., Philipov, P. P., and Koch, K.-W. (2002) *J. Biol. Chem.* **277,** 50365–50372
36. Senin, I. I., Vaganova, S. A., Weiergräber, O. H., Ergorov, N. S., Philippov, P. P., and Koch, K.-W. (2003) *J. Mol. Biol.* **330,** 409–418
37. Fischer, T., Senin, I. I., Philippov, P. P., and Koch, K.-W. (2002) *Spectroscopy* **16,** 271–279
38. Lambrecht, H.-G., and Koch, K.-W. (1992) *Biochim. Biophys. Acta* **1160,** 63–66
39. Hwang, J.-Y., Lange, C., Helten, A., Höppner-Heitmann, D., Duda, T., Sharma, R. K., and Koch, K.-W. (2003) *Eur. J. Biochem.* **270,** 3814–3821
40. Zozulya, S., and Stryer, L. (1992) *Proc. Natl. Acad. Sci. U. S. A.* **89,** 11569–11573
41. Otto-Bruc, A. E., Fariss, R. N., Van Hooser, J. P., and Palczewski, K. (1998) *Proc. Natl. Acad. Sci. U. S. A.* **95,** 15014–15019
42. Erickson, M. A., Lagnado, L., Zozulya, S., Neubert, T. A., Stryer, L., and Baylor, D. A. (1998) *Proc. Natl. Acad. Sci. U. S. A.* **95,** 6474–6479
43. Senin, I. I., Koch, K.-W., Akhtar, M., and Philippov, P. P. (2002) *Adr. Exp. Med. Biol.* **514,** 69–99
44. Makino, C. L., Dodd, R. L., Chen, J., Burns, M. E., Roca, A., Simon, M. I., and Baylor, D. A. (2004) *J. Gen. Physiol.* **123,** 729–741
45. Pulvermüller, A., Maretzki, D., Rudnicka-Nawrot, M., Smith, W. C., Palczewski, K., and Hofmann, K. P. (1997) *Biochemistry* **36,** 9253–9260
46. Calvert, P. D., Govardovskii, V. I., Krasnoperova, N., Anderson, R. E., Lem, J., and Makino, C. L. (2001) *Nature* **411,** 90–94